RSC Advances

ROYAL SOCIETY OF CHEMISTRY

www.rsc.org/advances

Synthesize of Ag-HNTs-MnO_2 Nanocomposites and Its Application for Nonenzymatic Hydrogen Peroxide Electrochemical Sensing

Sai Zhang, Qinglin Sheng and Jianbin Zheng*

Institute of Analytical Science, Shaanxi Provincial Key Laboratory of Electroanalytical Chemistry, Northwest University, Xi'an, Shaanxi 710069, China

Abstract: Natural halloysite nanotubes (HNTs) were attached to the flower-like MnO_2 and HNTs-MnO_2 composites were obtained, then silver nanoparticles were successfully deposited on the surface of HNTs-MnO_2 to produce Ag-HNTs-MnO_2 nanocomposites and they were used for fabricating nonenzymatic hydrogen peroxide (H_2O_2) sensor. Scanning electron microscopic, energy-dispersive X-ray spectrum, transmission electron microscope and Fourier transform infrared spectrum were applied to investigate the structures and morphologies of the resultant samples. The Ag-HNTs-MnO_2 composite-based modified electrode exhibited high eletrocatalytic activity to the reduction of H_2O_2 with a linear range of 2.0 μM to 4.71 mM, a detection limit of 0.7 μM (S/N = 3) and a sensitivity of 11.9 μA mM^{-1} cm^{-2}. In addition, high specific surface area, low cost and good biocompatibility made the modified electrode have a bright perspective in biosensors and biocatalysis.

Keywords: Nonezymatic sensor; MnO_2; Halloysite nanotubes; Hydrogen peroxide

1. Introduction

Accurate detection of hydrogen peroxide (H_2O_2) became increasingly important because it can not only serve as an oxidizing agent in a general industrial process, but also have a great significance for food, industrial, pharmaceutical, clinical and environmental analysis [1-4]. Among the techniques for the detection of H_2O_2, including spectrophotometry [5], titrimetry [6], chromatography [7], electrochemistry [8], and chemiluminescence [9, 10], electrochemical technique based on a simple and low cost electrode has been extensively applied for the detection of H_2O_2 [11-13]. Traditionally, the electrochemical sensor includes enzyme sensors and non-enzyme sensors. Although, many enzymatic H_2O_2 assays possess good sensitivity and selectivity, they are environmentally unstable and comparatively expensive [14].

* Corresponding author. Tel & Fax: +86 29 88303448.
E–mail: zhengjb@nwu.edu.cn

Compared with enzymatic H_2O_2 assays, nonenzymatic assays that employ metal oxides and their composites are more stable, very easy to synthesize, quite cost effective, even at high temperature and needs very less maintenance [15, 16]. In the light of these characteristics, how to develop enzyme-free H_2O_2 sensors with low detection limit and wide responding range have been paid increasing attention.

Nowadays, with the development of nanotechnology, metal nanoparticles (NPs) have been widely used to fabricate enzyme-free H_2O_2 sensors due to their unique properties of biocompatibility, catalysis and low toxicity. As a typical nanomaterial, silver nanoparticle (Ag NP) exhibits excellent physicochemical properties and shows good catalytic activity toward the reduction of H_2O_2 [17, 18]. For these reasons, many researchers have been synthesized silver nanoparticles to fabricate H_2O_2 sensors. Ag NPs and multiwalled carbon nanotubes were combined by Li, and the obtained functionalized composites were applied to fabricate a novel nonenzymatic H_2O_2 sensor [19]. Lu et al. synthesized multilayer films of polyelectrolyte/Ag NPs through the method of layer-by-layer self-assembling for enzymeless H_2O_2 sensing [20]. Wang et al. prepared nonenzymatic hydrogen peroxide sensor based on the electrodeposition of silver nanoparticles on poly (ionic liquid)-stabilized graphene sheets [21].

In view of the above researches, it can be seen that homogeneously dispersed silver nanoparticles are extremely significant in fabrication of H_2O_2 sensors and some available substrates are necessary to prevent the aggregation of Ag NPs. Commonly used materials include carbon nanomaterials, metallic oxide and polymeric membrane et al. [19-21]. Nowadays, metallic oxides (TiO_2 [22], SiO_2 [23], CuO [24], Fe_3O_4 [25], etc.) which display a lot of advantages such as low cost, simple synthesis, unique electrochemical and optic properties have been attracted much attentions. Among them, manganese dioxide (MnO_2) is considered as one of the candidates on account of its low cost, high energy density, environmental pollution-free and nature abundance. Several kinds of MnO_2 nanomaterials have been utilized in fabrication of electrochemical sensors [26-28]. As we known, due to the basic unit MnO_6 octahedral is linked in different ways of MnO_2 [29], it have some crystallographic forms in nature (such as α, β, γ, and δ). Different from (1D) MnO_2 nanostructures, it is not easy to obtain two- and three-dimensional (2D and 3D) ordered nanostructured MnO_2

semiconducting materials though they are urgent need for advanced optoelectronic, information storage and nanoscale electronic applications [30]. Through our tireless efforts, a facile one-step solution phase shape-controlled of 3D hierarchical nanostructures of MnO_2 synthetic approach at room temperature have been researched and it could overcome this problem primely. It is obviously to see that the method is environmentally friendly, which could be regard as a promising green chemical synthesis in widespread practical applications. However, the application of 3D MnO_2 was quite few in contrast with 1D MnO_2 and 2D MnO_2 and few researchers have been paid attention to the application to electrochemistry of 3D MnO_2. We think it may have a good exhibition in the areas of sensor for its high specific surface of hierarchical nanostructures. In this work, we employ (3D) MnO_2 as a catalyst support. The specific flower-like structure is formed by soft silk films with wrinkle which looks like the structure of monolayer grapheme and the high surface-to-volume ratio of flower-like MnO_2 can provide large interspaces for the immobilization of Ag NPs [31], thus preventing the aggregation of silver nanoparticles effectively and obtaining highly dispersed silver nanoparticles, achieving faster electron transfer, promoting the property of constructed H_2O_2 sensors. In view of the above mentioned points, the research on (3D) MnO_2 nanomaterials seems to be a hot pot for their alternation of other noble metals in the area of electrocatalysis. To further increase the amount of adsorbed metal particles, making the surface of flower-like MnO_2 rougher so that the nanocomposites could play the greatest potential to improve the detection performance of the sensor towards H_2O_2, the activity of Ag-MnO_2 for H_2O_2 reduction needs to be further enhanced.

Recently, Halloysite nanotubes (HNTs) have been aroused much attention as an immobilization matrix for biosensors and biocatalysis [32]. They are naturally occurring alumi-nosilicates ($Al_2Si_2O_5(OH)_4 \cdot$ nH2O) with a regular nanotubular bulk structure, morphology, rich mesopores and nanopores. The size of halloysite nanotubes varies from 50 to 70 nm in external diameter, 15 nm diameter lumen and 1±0.5 μm length. Due to the siloxane and a few hydroxyl groups occupied the outer surfaces of HNTs, HNTs could disperse in solution more uniformly than other natural

silicates (such as kaolinite and montmorillonite) and possess the unique property to form hydrogen bonding [33]. Different from other layered silicates, the reason of easily dispersion on halloysites was that their infirm secondary interactions among the nanotubes via Vander Waals forces and hydrogen bonds [34].In addition, the naturally occurring HNTs are much cheaper and easily available. Compared to carbon nanotubes (CNTs), HNTs were selected as reliable substrates in many scopes due to their unique characteristics, such as different outside and inside chemistry and adequate hydroxyl groups on the surface of HNTs. [35]. Considering its special performance, we would disperse it on the flower-like MnO_2. In terms of the nanocomposites, not only the MnO_2 own the ability to catalyze hydrogen peroxide, but also the HNTs nanotubes could increase the surface area of flower-like MnO_2, creating favorable conditions for a large number of silver nanoparticles adsorption.

The aim of the present work is to synthesize Ag-HNTs-MnO_2 nanocomposites by employing reduction reaction and ultrasonic agitation, fabricating a novel non-enzymatic sensor of H_2O_2 based on the unique material by simple cast method and used for sensitively detect H_2O_2.

Experimental

1.1 Materials

Halloysite nanotubes were purchased from Natural Nano. Inc. Chitosan (CS, MW5-6×10^5, >90% deacetylation) was got from Shanghai Yuanju Biotechnology Co, Ltd (shanghai, China). H_2O_2 (30%, v/v aqueous solution) was purchased from Tianjin Tianli Chemistry Reagent Co., Ltd (Tianjin, China). 0.1 M phosphate buffered saline (PBS, pH 7.2). All other chemicals and reagents were of analytical reagent grade and deionized water was used in experiments.

1.2 Apparatus and electrochemical measurements

Scanning electron microscope (SEM) and energy dispersive spectroscopy (EDS) were got with a JSM-6390F scanning electron microscope (JEOL, Japan). Transmission electron microscopy (TEM) patterns were done on a JEM-2100 scanning electron microscope (JEOL, Japan). All of the electrochemical measurements were obtained on a CHI 660 electrochemical analyzer (Shanghai Chenhua Instrument Co. Ltd., China). A conventional three-electrode cell was used, including a platinum wire as counter electrode, a saturated calomel electrode (SCE) as

reference electrode, and the modified glassy carbon electrodes (GCE, 3mm in diameter) as working electrode. The analytical solutions were purged with highly purified nitrogen for at least 30 minutes before electrochemical experiments and maintained under nitrogen atmosphere during the experiments. All the measurements were conducted at room temperature (25 ± 2 °C).

2.3. Preparation of the sensor

2.3.1. Sythesis of HNTs-MnO_2

In a typical synthesis, 200 mL of manganous chloride ($MnCl_2$) solution (20 mM) was mixed with ethylenediaminetatraacetic acid disodium salt (EDTA) solution. 80 mg HNTs we dispersed in the above solution under sonication. After sonicating for 1 h, 200 mL of sodium hydroxide (250 mM) was added to the system. Then, 200 mL of potassium persulfate ($K_2S_2O_8$) was added to initiate the redox reaction. After standing at 30°C for overnight, the solid product was collected by filtration, washed with doubly distilled water and finally with ethanol, followed by vacuum drying at 80 °C. The obtained sample was denoted as HNTs-MnO_2.

2.3.2. Synthesis of Ag-HNTs-MnO_2

HNTs-MnO_2 powder (10 mg) was dispersed in 50 mL ethanol-water (1:1, v/v ratio) solution, ultrasonically mixed with 2.0 mL of 0.1 mM $AgNO_3$ solution, and subsequently added excess $NaBH_4$ solution in a dropwise manner under stirring condition. The reductive reaction was performed under room temperature for 2 h with continuous magnetic stirring, after which, the composite products were separated from the solution in a centrifuge, ultrafiltration and thoroughly washed with doubly distilled water. The obtained black powder was dried in a vacuum oven at 70°C for 12 h. For comparison, Ag-MnO_2 and HNTs-MnO_2 were prepared by the same process.

2.3.3. Electrode modification

The glass carbon electrode (GCE) was prepared by a simple casting method. Prior to use, the GCE was polished with 1.0 and 0.3 μm alumina powder to obtain mirror like surface, respectively, and rinsed with doubly distilled water, followed by sonication in ethanol solution and doubly distilled water successively. Then, the GCE was allowed to dry in a stream of nitrogen. The composites (5 mg) were dispersed into chitosan (5 mL, 0.5 %) and sonicated for 30 minutes; suspension (5 μL) was cast onto the GCE and then dried in air at room temperature. The resulted electrode was denoted as Ag-HNTs-MnO_2/GCE.

2. Results and Discussion

2.1 Characterization of Ag-HNTs-MnO_2 nanocomposites

The morphologies and structure of the MnO_2, HNTs, MnO_2-HNTs and Ag-HNTs-MnO_2 were characterized by SEM and TEM as shown in Fig. 1. An overall view in Fig. 1A indicates many flower-like nanoarchitectures. The high-magnification image in Fig. 1B shows that a double flowery nanostructure is made of tiny nanopetals growing outside from different sites. An obvious phenomenon was worth mentioning that although suffer from long-time sonication, the new-get nanostructure cannot be destroyed into discrete petals, suggesting that the nanocomposites are actually integrated tightly rather than delicate aggregates. From Fig. 1C and Fig. 1D, it can be seen that HNTs are the tubular structures of hollow and open-ended in the submicrometer range. Commonly, the size of HNTs varies from 1200 to 500 nm in length, with the internal diameter of ~15 nm and the outer diameter of ~100 nm. Fig. 1E showed that the vast majority of HNTs were coated with flower-like MnO_2, and almost no parts of the HNTs were naked, implying the strong binding between HNTs and MnO_2. It can be seen clearly from Fig. 1F that HNTs nanotubes loaded onto the MnO_2 sheet thus could further enhance the active surface area of MnO_2 and adsorb more silver nanoparticles. Fig. 1G and Fig. 1H showed that granular nanosilver attached on MnO_2 surfaces without any Ag NPs aggregation.

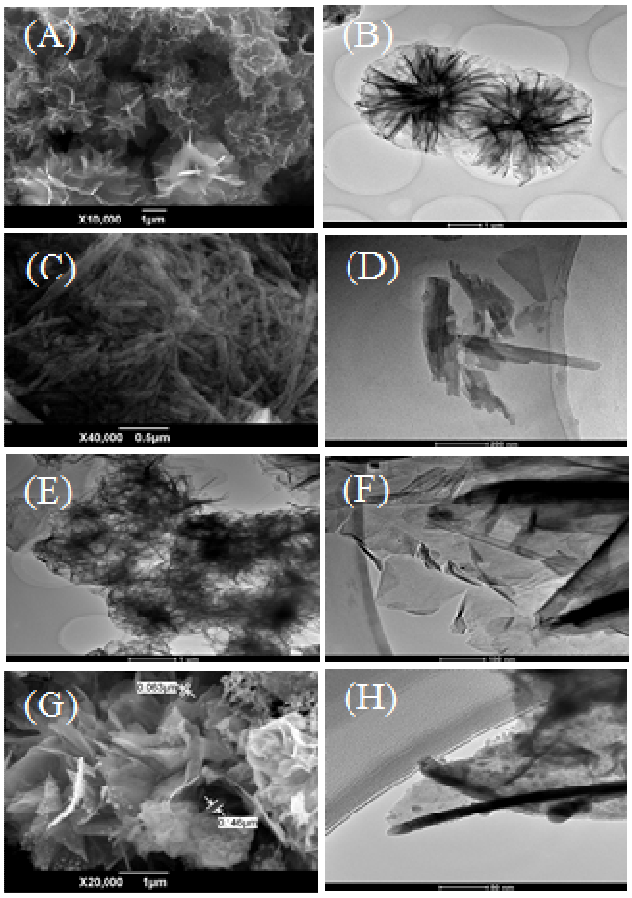

Fig. 1 TEM and SEM images of nanocomposites: (A, B) MnO_2, (C, D) HNTs, (E, F) HNTs-MnO_2 and (G, H) Ag-HNTs-MnO_2

Fig. 2 showed the EDS patterns of HNTs-MnO_2 and Ag-HNTs-MnO_2. From Fig. 2A and 2B, the EDS patterns revealed that the nanocomposites were composed of O, Al, Mn and Ag elements, suggesting that HNTs-MnO_2 and Ag-HNTs-MnO_2 nanocomposites had been synthesized successfully.

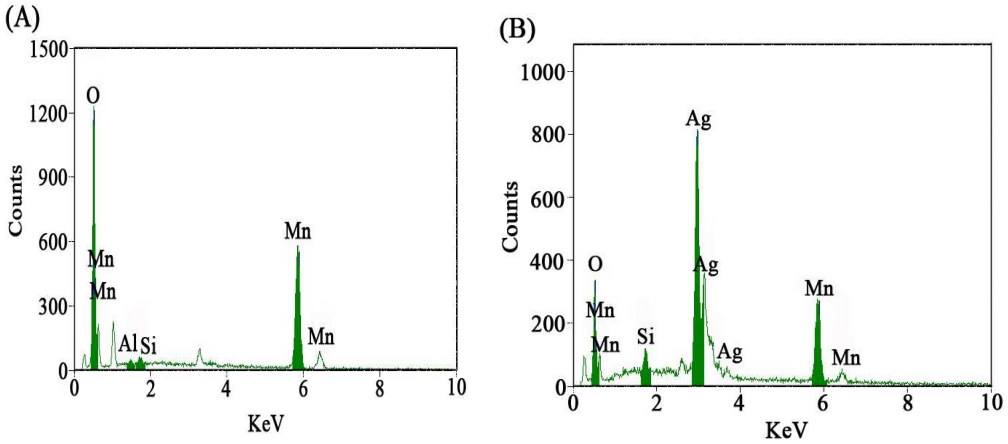

Fig. 2 EDS spectrum of (A) HNTs-MnO_2 and (B) Ag-HNTs-MnO_2 nanocomposites

FTIR spectra were helpful to further understand the formation of nanocomposites. Fig. 3a showed that four peaks present in the FTIR spectrum of HNTs. Double peaks at 3697 and 3622 cm^{-1} appeared on the spectrum of HNTs (curve a), which were due to the stretching vibrations of hydroxyl groups at the surface of HNTs. The peaks about 1000 cm^{-1} were assigned to Si-O groups in HNTs. In addition, a single Al_2OH bending band at 916 cm^{-1}, and a band at 1022 cm^{-1} attributed to Si-O-Si stretching vibrations. Compared with HNTs, the other two peaks of HNTs-MnO_2 (curve b) were observed at 1600 cm^{-1} and 545 cm^{-1}.The peak at 1600 cm^{-1} was related to water -OH bending and the peak at 545 cm^{-1} should be ascribed to the Mn-O and Mn-O-Mn vibrations in [MnO_6] octahedral. After metallic Ag (curve c) particles were loaded, the final nonocomposites exhibit low absorption-peak intensity of the functional group; the main reason was that once Ag nanoparticles existencing, the absorption peak of MnO_2 was covered.

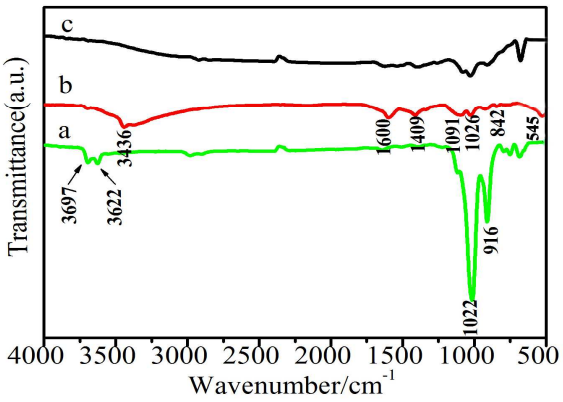

Fig. 3 FTIR spectra of (a) HNTs, (b) HNTs-MnO_2 and (c) Ag-HNTs-MnO_2 nanocomposites

3.3. Electrochemical properties of Ag-HNTs-MnO_2

Electrochemical impedance spectroscopy (EIS) can study the interfacial properties of surface-modified electrodes usefully. As we known, the semicircle diameter equaled to the electron transfer resistance (R_{et}). We can seen from Fig. 4, the value of R_{ct} is increased from 1750 Ω (curve c) to 2300 (curve b) after introducing HNTs onto the MnO_2 modified electrode while the value is decreased to 500 Ω after introducing AgNPs (curve a). These results suggest that after MnO_2 was modified on GCE, electron transfer between the solution and the electrode is less efficient which is ascribed to the semiconductive of MnO_2 nanoflowers. When HNTs is immobilized

onto electrode, a remarkable increase in the semicircle diameter was observed due to the poor electric conductivity of HNTs, after Ag is immobilized onto electrode, the electron transfer resistance value is reduced owing to the good conductivity of Ag NPs that decreased the impedance of the electrode. The results were indicating that the Ag-HNTs-MnO_2 could efficiently enhance the electron transfer.

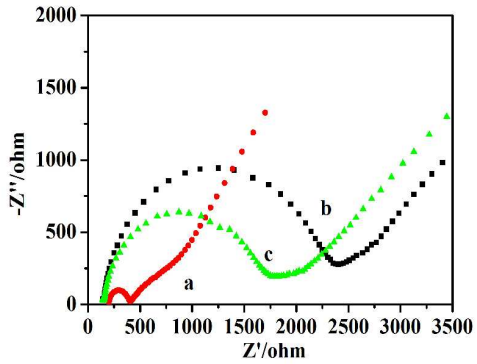

Fig. 4 EIS of (a) Ag-HNTs-MnO_2/GCE, (b) HNTs-MnO_2/GCE, (c) MnO_2/GCE HNTs/GCE in 5.0 mM $[Fe(CN)_6]^{4-/3-}$ containing 0.1 M KCl from 10^5 to 10^{-2} Hz at amplitude of 5 mM

Fig. 5 recorded cyclic voltammograms (CVs) in N_2-saturated 0.1 M PBS (pH 7.2) of the bare GCE (a, b), HNTs-MnO_2/GCE (c, d) and the Ag-HNTs-MnO_2/GCE (e, f) at a scan rate of 100 mVs^{-1} in 0.1 M PBS. Bare GCE (a), HNTs-MnO_2/GCE (c) and the Ag-HNTs-MnO_2/GCE (e) showed weak electrochemical response in the absence of H_2O_2. After adding 1.0 mM H_2O_2, the electrochemical responses were increased accordingly. However, compared with bare GCE (b), HNTs-MnO_2/GCE (d), Ag-HNTs-MnO_2/GCE (curve f) exhibited greatly current response about 8.5 μA in intensity at –0.65 V, indicating that the Ag NPs exhibited excellent catalytic performance toward H_2O_2.

Accroading to the literature [36], the catalytic mechanism proposed for the reduction of H_2O_2 was as follows:

$$H_2O_2 + e^- \rightleftharpoons OH\ (ad) + OH^-$$

$$OH\ (ad) + e^- \rightleftharpoons OH^-$$

$$2OH^- + 2H^+ \rightleftharpoons 2H_2O$$

When the Ag NPs were deposited on the electrode, the reaction became more irreversible [36]:

$$H_2O_2 \xrightarrow{Ag} \frac{1}{2}O_2 + H_2O$$

$$O_2 + 2e^- + 2H^+ \xrightarrow{GCE} H_2O_2$$

Then the O_2 generated in the action above would turn into the detection signal on electrode. It had been proposed [37] that the electroreduction of oxygen on electrode occurred via the mechanism shown below [38]:

$$O_2 + e^- \rightleftharpoons [O_2^{\cdot -}] \text{ (ads)}$$

$$[O_2^{\cdot -}] \text{ (ads)} + H_2O \rightleftharpoons HO_2^{\cdot -}\text{(ads)} + OH^-$$

Then

$$HO_2^{\cdot -}\text{(ads)} + O_2^- \rightleftharpoons HO_2^- \text{(aq)} + O_2$$

Or

$$HO_2^{\cdot}\text{(ads)} + e^- \rightleftharpoons HO_2^-\text{(aq)}$$

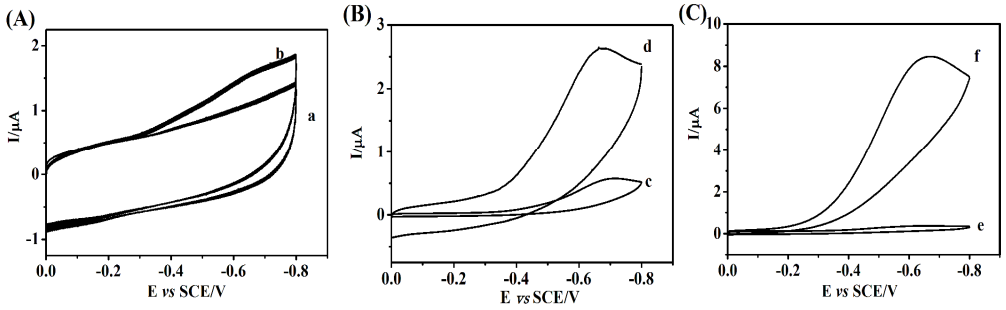

Fig. 5 CVs of bare GCE (A), HNTs-MnO_2/GCE (B), Ag-HNTs-MnO_2/GCE (C) in N_2-saturated 0.1 M PBS in the absence (a, c and e) and presence (b, d and f) of 1.0 mM H_2O_2

With bring Ag NPs modified onto the HNTs-MnO_2 electrode, the detection signal of H_2O_2 was amplified. There are some rational reasons could be considered: Firstly, flower-like MnO_2 layer can provide roomy space for Ag NPs adsorption, thus obtain more electroactive sites. Secondly, in terms of MnO_2 smooth surface, the rough HNTs could further support high surface area for nanoparticles loading to keep the high catalytic activity. Thirdly, HNTs lives as a natural holder, increase the effective surface area of unique morphology MnO_2, with homogeneous Ag NPs, they all have the good ability to catalyze H_2O_2, once integrate there own unique properties, a new designed nanocomposites sensor will present excellent performance towards catalyzing.

The catalytic activity of Ag-HNTs-MnO_2 nanocomposites by changing the

concentration of H_2O_2 was shown in Fig. 6A. It can be seen that no characteristic peak was shown when no H_2O_2 was introduced into the system. After injecting H_2O_2 into the N_2-saturated 0.1 M PBS (pH 7.2), a gradually increased reduction current appeared, indicating the final nanocomposite own the excellent response and electrocatalytic activity towards H_2O_2. It was notable that with the increment of H_2O_2 concentration, the reduction current gradually increased. From Fig. 6B we can get the effect of potential scan rate on peak current of Ag-HNTs-MnO_2. The cathodic peak current increased in a linear relationship with the square root of with increasing the scan rates from 20 to 140 $mV \cdot s^{-1}$, indicating that the reactions occurring on the modified electrode were irreversible and this process was diffusion-controlled.

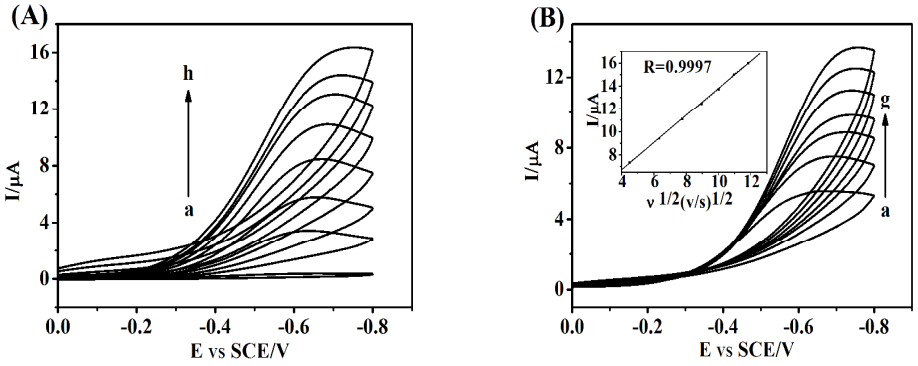

Fig. 6 (A) CVs of the Ag-HNTs-MnO_2/GCE in N_2-saturated 0.1M PBS (pH 7.2) in the absence and presence of H_2O_2 with different concentrations (from a to g: 0, 1, 2, 3, 4, 5 , 6 and 7 mM at the scan rate of 100 mV/s). (B) CVs of the Ag-HNTs-MnO_2/GCE N_2-saturated 0.1M PBS (pH 7.2) containing 5.0 mM H_2O_2 at different scan rates (from a to g: 20, 40, 60, 80, 100, 120 and 140 mV/s). Inset: plot of electrocatalytic peak current of H_2O_2 versus $\upsilon^{1/2}$

Fig. 7A showed a typical amperometric response curve of H_2O_2 at Ag-HNTs-MnO_2/GCE in N_2-saturated 0.1 M PBS (pH 7.2) for the different concentrations of H_2O_2. We can observe a stable, well-defined and fast amperometric response under successive step additions of H_2O_2. Although the modified electrode exhibited biggest catalytic activity at −0.65 V, the background was much too high to interfere the detection. So detect H_2O_2 was carried out at −0.3 V to ensure a low applied potential, good signal-to-noise ratio and less interference of other electroactive species in the solution. It was clear that the response current of the modified electrode increased to steady-state values less than 2 s upon the addition of H_2O_2, indicating a fast amperometric response behavior. Fig. 7B showed the

calibration curve for the H_2O_2. With increasing add H_2O_2, the working electrode gave a linear dependence in the H_2O_2 concentration range of 2.0 μm to 4.71 mM and the linear regression equation was expressed as I_p (μA) = 1.03+8.45·C (mM) with a correlation coefficient of 0.9996, a sensitivity of 11.9 μA mM^{-1} cm^{-2} and a detection limit of 0.7 μM at a signal-to-noise ratio of 3. These results indicated that the Ag-HNTs-MnO_2/GCE can be used for the preparation of an amperometric sensor for H_2O_2 with quick response and wide linear range, deeply illustrate this new sensor own excellent property.

As shown in Table 1, several typical non-enzymatic and enzymatic H_2O_2 sensors reported previously have been compared. We can observe that the wide linear range, the low detection limit and the short response time due to the high surface-to-volume ratio and larger surface area for H_2O_2 molecules adsorb and react. The unique morphology of MnO_2 provides larger surface and effective surface area for the attachment of Ag NPs. In addition, Ag NPs and flower-like MnO_2 are also acts the role of the electron transfer promoter. As a result, the new construct nanocomposites can be used for detecting H_2O_2 efficiently.

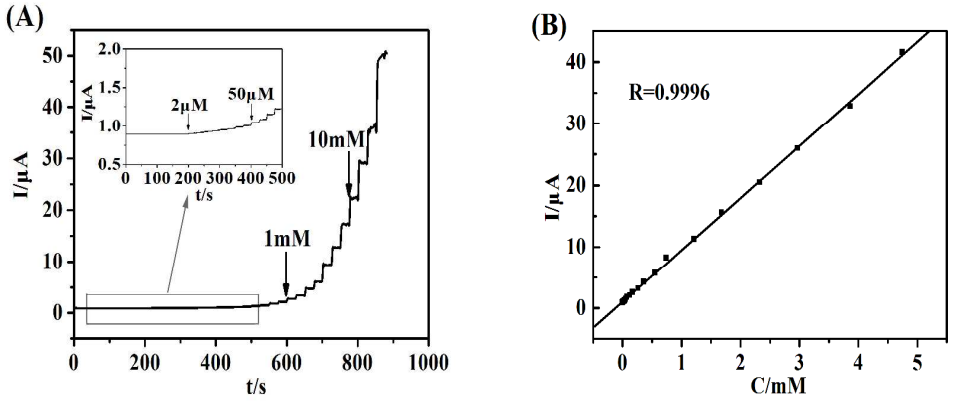

Fig. 7 (A) Typical amperometric response of the Ag-HNTs-MnO_2/GCE on successive injection of H_2O_2 into the stirring N_2-saturated 0.1 M PBS (pH 7.2), applied potential: −0.3 V. (B) Calibration curve of H_2O_2 versus its concentration

Table. 1 Comparison of several typical nonenzymatic H_2O_2 sensors

Sensors	Linear range (mM)	Sensitivity (μA mM^{-1} cm^{-2})	Detection limit (μM)	Literature
MnO_2/GO/GCE	0.005–0.6	-	0.8	[39]
MnO_2/carbon fiber	0.01-0.26	10.6	5.4	[40]

(DNA-AgNCs)/GE	0.02-23	-	3	[41]
Platinum hierarchical nanoflowers	0.01-4.0	1.39	1.05	[42]
AgNP/SnO_2	0.01–3.5	-	5.0	[43]
PtAu/G-CNTs	0.002-8.6	-	0.6	[44]
Ag-HNTs-MnO_2	0.002-4.71	11.9	0.7	This work

3.4. Interference study

In terms of non-enzyme H_2O_2 sensor, good selectivity is very important. Under the optimized experimental conditions, some potential interfering species such as ascorbic acid (AA), uric acid (UA), glucose, and acetaminophen (AP) have been investigated. As shown in Fig. 8 (A), H_2O_2 solution was firstly injected into the N_2-saturated 0.1 M PBS (pH 7.2) at a working potential of −0.3 V, and followed by the addition of interferences (0.01 mM, respectively). It can be seen that an obvious amperemetric response appeared at once 0.1 mM H_2O_2 were injected while Ascorbic acid (AA), acetaminophen (AP), glucose (Glu) did not cause any further amperometric changes. The result indicates that the modified electrode exhibited good ability of anti-interference to electroactive species, which attribute to the relatively lower potential at −0.3 V. The interfering species of oxygen were also investigated by testing the amperometric responses of H_2O_2 at the same potential. As seen from Fig. 8 (B), a stable response current and good signal-to-noise ratio can be observed in N_2-saturated 0.1 M PBS at −0.3 V (curve b). In O_2-saturated 0.1 M PBS at −0.3 V (curve a), although the background noise increased due to the electro-reduction of O_2, the response currents almost remained unchanged, meaning the resulting electrode exhibited good ability of anti-interference to O_2.

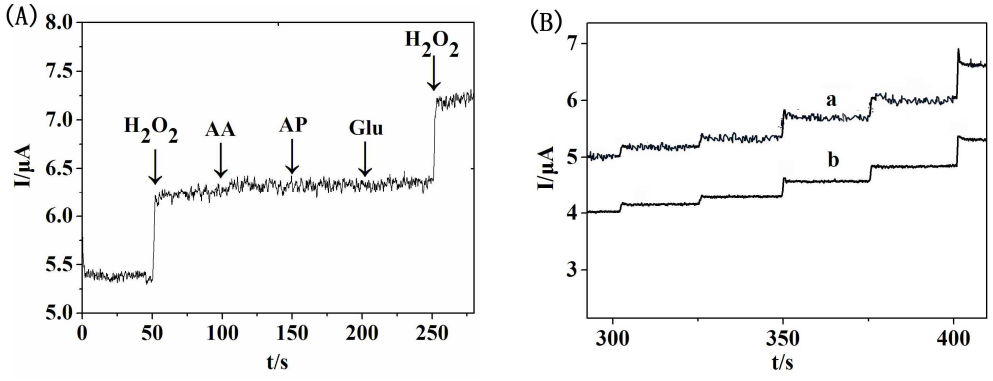

Fig. 8 Amperometric response of the Ag-HNTs-MnO_2/GCE to (A) successive addition of H_2O_2, AA, AP, Glu (0.05 mM, respectively) in N_2-saturated 0.1 M PBS (pH 7.2) at −0.3 V and (B) successive addition of H_2O_2 (0.05 mM) in (a) O_2-saturated and (b) N_2-saturated 0.1 M PBS (pH 7.2) at −0.3 V

3.5. Repeatability and stability

The repeatability and stability of the resulted H_2O_2 sensors were also investigated. There are four Ag-HNTs-MnO_2 modified electrodes were investigated at the same condition to compare their amperometric current responses. The result suggests that the relative standard deviation for current determination of H_2O_2 was 3.5%, confirming that the Ag-HNTs-MnO_2/GCE nanocomposite modified electrode was highly reproducible. The stability of the modified GCE was also estimated every one week, founding the modified electrode remained 90% of its initial current response. Thus, the modified GCE processed acceptable repeatability and stability.

4. Conclusion

In summary, Ag-HNTs-MnO_2 nanocomposites had been synthesized successfully by a facile simple strategy and a novel non-enzymatic H_2O_2 sensor based on the nanocomposites was fabricated. The novel sensor exhibits good electrocatalytic activities toward H_2O_2 reduction, low detection limit, long-time stability and high response sensitivity, indicating its prominent electrochemical behavior towards electroactive biomolecules. Extraordinary, flower-like MnO_2 provides more binding sites for Ag NPs to enhance the catalyst ability, making the performance of the proposed modified electrode more effectively. Finally, we believe that the type of high-performance nanostructured sensor, combined with a low-cost and scalable technique could be used as promising platform for the construction of various nonenzymatic electrochemical sensors for further study.

Acknowledgments

The authors gratefully acknowledge the financial support of this project by the Specialized Research Fund for the Doctoral Program of Higher Education (No. 20126101120023), National Science Fund of China (No. 21275116), the Fund of Shaanxi Province Educational Committee of China (No. 12JK0576), the Scientific Research Foundation of Shaanxi Provincial Key Laboratory (11JS080, 12JS087, 13JS097, 13JS098), the Natural Science Foundation of Shaanxi Province in China (No. 2012JM2013, No. 2013KJXX-25).

References

[1] Butwong N, Zhou L, Ng-eontae W, et al. A sensitive nonenzymatic hydrogen peroxide sensor using cadmium oxide nanoparticles/multiwall carbon nanotube modified glassy carbon electrode. J Electroanal Chem. 2014; 717-718: 41-6.

[2] Babu KJ, Zahoor A, Nahm KS, et al. The influences of shape and structure of MnO_2 nanomaterials over the non-enzymatic sensing ability of hydrogen peroxide. J Nanopart Res. 2014; 16(2): 1-10.

[3] Jia NM, Huang BZ, Chen L, et al. A simple non-enzymatic hydrogen peroxide sensor using gold nanoparticles-graphene-chitosan modified electrode. Sens Actuators B. 2014; 195: 165-70.

[4] Han Q, Ni PJ, Liu ZR, et al. Enhanced hydrogen peroxide sensing by incorporating manganese dioxide nanowire with silver nanoparticles. Electrochem Commun. 2014; 38: 110-3.

[5] Ghaderi S and Mehrgardi MA. Prussian Blue-Modified Nanoporous Gold Film Electrode for Amperometric Determination of Hydrogen Peroxide. Bioelectrochem. 2014; 98: 64-9.

[6] Yang YJ, Li WK and Wu XM. Copper sulfide reduced graphene oxide nanocomposite for detection of hydrazine and hydrogen peroxide at low potential in neutral medium. Electrochim Acta. 2014; 123: 260-7.

[7] Eduardozapp, Nascimento V, Dambrowski D, et al. Bio-inspired sensor based on glutathione peroxidase mimetic for hydrogen peroxide detection. Sens Actuators B. 2013; 176: 782-8.

[8] Zhang LJ, Chen YC, Zhang ZM, et al. Highly selective sensing of hydrogen peroxide based on cobalt-ethylenediaminetetraacetate complex intercalated layered double hydroxide-enhanced luminol chemiluminescence. Sens Actuators B. 2014; 193: 752-8.

[9] Vdovenko MM, Demiyanova AS, Kopylov KE, et al. FeIII-TAML activator: A potent peroxidase mimic for chemiluminescent determination of hydrogen peroxide. Talanta 2014; 125: 361-5.

[10] Ensafi A, Abarghoui MM and Rezaei B. Electrochemical determination of hydrogen peroxide using copper/porous silicon based non-enzymatic sensor. Sens Actuators B. 2014; 196: 398-405.

[11] Doroftei F, Pinteala T and Arvinte A. Enhanced stability of a Prussian /sol-gel composite for electrochemical determination of hydrogen peroxide. Microchim Acta. 2014; 181(1-2): 111-20.

[12] Zhang LL, Han GQ, Liu Y, et al. Immobilizing haemoglobin on gold/graphene–chitosan nanocomposite as efficient hydrogen peroxide biosensor. Sens Actuators B. 2014; 197: 164-71.

[13] Mani V, Dinesh B, Chen S-M, et al. Direct electrochemistry of myoglobin at reduced graphene oxide-multiwalled carbon nanotubes-platinum nanoparticles nanocomposite and biosensing towards hydrogen peroxide and nitrite. Biosens Bioelectron. 2014; 53: 420-7.

[14] Mundaca-Uribe R, Bustos-Ramírez F, Zaror-Zaror C, et al. Development of a Bienzymatic Amperometric Biosensor to Determine Uric Acid in Human Serum, based on Mesoporous Silica (MCM-41) for Enzyme Immobilization. Sens Actuators B. 2014; 195: 58-62.

[15] Zhao W, Wang H, Qin X, et al. A novel nonenzymatic hydrogen peroxide sensor based on multi-wall carbon nanotube/silver nanoparticle nanohybrids modified gold electrode. Talanta 2009; 80(2): 1029-1033.

[16] Song MJ, Hwang S W, Whang D. Non-enzymatic electrochemical CuO nanoflowers sensor for hydrogen peroxide detection. Talanta 2010; 80(5): 1648-1652.

[17] Liao KM, Mao P, Li YH, et al. A promising method for fabricating Ag nanoparticle modified nonenzyme hydrogen peroxide sensors. Sens Actuators B. 2013; 181: 125-9.

[18] Liu RX, Wei YH, Zheng JB, et al. A Hydrogen Peroxide Sensor Based on Silver Nanoparticles Biosynthesized by Bacillus subtilis. Chin J Chem. 2013; 31(12): 1519-25.

[19] Li XY, Liu YX, Zheng LC, et al. A novel nonenzymatic hydrogen peroxide sensor based on silver nanoparticles and ionic liquid functionalized multiwalled carbon nanotube composite modified electrode. Electrochim Acta. 2013; 113: 170-5.

[20] Lu WB, Luo YL, Chang GH, et al. Layer-by-layer self-assembly of multilayer films of polyelectrolyte/Ag nanoparticles for enzymeless hydrogen peroxide detection. Thin Solid Films. 2011; 520(1): 554-7.

[21] Wang Q and Yun YB. Nonenzymatic sensor for hydrogen peroxide based on the electrodeposition of silver nanoparticles on poly (ionic liquid)-stabilized graphene sheets. Microchim Acta. 2013; 180(3-4): 261-8.

[22] Li DW, Pan LJ, Li S, et al. Controlled preparation of uniform TiO_2-catalyzed

silver nanoparticle films for surface-enhanced Raman scattering. J Phys Chem C. 2013; 117(13): 6861-71

[23] Lu L, Qian YX, Wang LH, et al. Metal-Enhanced Fluorescence-Based Core–Shell Ag@SiO2 Nanoflares for Affinity Biosensing via Target-Induced Structure Switching of Aptamer. ACS Appl Mater Inter. 2014; 6(3): 1944-50.

[24] Gao SY, Li ZD, Jiang K, et al. Biomolecule-assisted in situ route toward 3D superhydrophilic Ag/CuO micro/nanostructures with excellent artificial sunlight self-cleaning performance. J Mater Chem. 2011; 21(20): 7281-8.

[25] Du JJ and Jing CY. Preparation of Thiol Modified Fe_3O_4 @ Ag Magnetic SERS Probe for PAHs Detection and Identification. J Phys Chem C. 2011; 115(36): 17829-35.

[26] Han Y, Zheng JB and Dong SY. A novel nonenzymatic hydrogen peroxide sensor based on Ag-MnO_2-MWCNTs nanocomposites. Electrochim Acta. 2013; 90: 35-43.

[27] Zhou DL, Chen D, Zhang PP, et al. Facile synthesis of MnO_2–Ag hollow microspheres with sheet-like subunits and their catalytic properties. CrystEngComm 2014; 16(5): 863-9.

[28] Han Q, Ni P, Liu Z, et al. Enhanced hydrogen peroxide sensing by incorporating manganese dioxide nanowire with silver nanoparticles. Electrochemistry Communications 2014; 38: 110-113.

[29] Cheng F, Zhao J, Song W, et al. Facile controlled synthesis of MnO_2 nanostructures of novel shapes and their application in batteries. Inorganic chemistry 2006; 45(5): 2038-2044.

[30] Ng H T, Li J, Smith M K, et al. Growth of epitaxial nanowires at the junctions of nanowalls. Science 2003; 300(5623): 1249-1249.

[31] Zhang JT, Guo CX, Zhang LY, et al. Direct growth of flower-like manganese oxide on reduced graphene oxide towards efficient oxygen reduction reaction. Chem. Commun. 2013; 49(56): 6334-6.

[32] Chao C, Liu JD, Wang JT, et al. Surface Modification of Halloysite Nanotubes with Dopamine for Enzyme Immobilization. ACS Appl Mater Inter. 2013; 5(21): 10559-64.

[33] Yuan P, Southon PD, Liu ZW, et al. Functionalization of Halloysite Clay Nanotubes by Grafting with γ-Aminopropyltriethoxysilane. J Phys Chem C. 2008; 112 (40): 15742–51.

[34] Lecouvet B, Sclavons M, Bourbigot S, et al. Water-assisted extrusion as a novel processing route to prepare polypropylene/halloysite nanotube nanocomposites: structure and properties. Polymer. 2011; 52(19): 4284-95.

[35] Liu RC, Zhang B, Mei DD, et al. Adsorption of methyl violet from aqueous solution by halloysite nanotubes. Desalination 2011, 268(1): 111-116.

[36] Honda M, Kodera T and Kita H. Electrochemical behavior of H_2O_2 at Ag in $HClO_4$ aqueous solution. Electrochim Acta. 1986; 31(3): 377-83.

[37] Downard AJ. Electrochemically assisted covalent modification of carbon electrodes. Electroanalysis 2000; 12(14): 1085-96.

[38] Šljukić B, Banks CE and Compton RG. An overview of the electrochemical reduction of oxygen at carbon-based modified electrodes. J Iran Chem Soc. 2005; 2(1): 1-25.

[39] Li L, Du Z, Liu S, et al. A novel nonenzymatic hydrogen peroxide sensor based on MnO_2 graphene oxide nanocomposite. Talanta 2010; 82(5): 1637-1641.

[40] Hocevar SB, Ogorevc B, Schachl K, et al. Glucose microbiosensor based on MnO_2 and glucose oxidase modified carbon fiber microelectrode. Electroanalysis 2004; 16(20): 1711-6.

[41] Xia YL, Li WH, Wang M, et al. A sensitive enzymeless sensor for hydrogen peroxide based on the polynucleotide-templated silver nanoclusters/graphene modified electrode. Talanta 2013; 107: 55-60.

[42] Heli H, Sattarahmady N, Dehdari Vais R, et al. Enhanced electrocatalytic reduction and highly sensitive nonenzymatic detection of hydrogen peroxide using platinum hierarchical nanoflowers. Sens Actuators B. 2014; 192: 310-6.

[43] Miao Y- E, He SX, Zhong YL, et al. A novel hydrogen peroxide sensor based on Ag/SnO_2 composite nanotubes by electrospinning. Electrochim Acta. 2013; 99: 117-23.

[44] Lu DB, Zhang Y, Lin SX, et al. Synthesis of PtAu bimetallic nanoparticles on graphene–carbon nanotube hybrid nanomaterials for nonenzymatic hydrogen peroxide sensor. Talanta 2013; 112: 111-6.